



# A Fourier transform spectroradiometer for ground-based remote sensing of the atmospheric downwelling long-wave radiance

Giovanni Bianchini<sup>1</sup>, Francesco Castagnoli<sup>1</sup>, Gianluca Di Natale<sup>1</sup>, and Luca Palchetti<sup>1</sup>

<sup>1</sup>Consiglio Nazionale delle Ricerche, Istituto Nazionale di Ottica, Via Madonna del Piano 10, 50019 Sesto Fiorentino, Italy

**Correspondence:** Giovanni Bianchini ([giovanni.bianchini@ino.cnr.it](mailto:giovanni.bianchini@ino.cnr.it))

**Abstract.** The Radiation Explorer in the Far Infrared - Prototype for Applications and Development (REFIR-PAD) is a Fourier transform spectroradiometer that has been designed to operate both from stratospheric balloon platform and from ground. It has been successfully deployed in a stratospheric balloon flight and several ground based campaigns from high altitude sites, including the current installation in the Concordia Italian-French Antarctic station. The instrument is capable to operate autonomously with only a limited need of remote control and monitoring, and is providing a multi-year dataset of spectrally resolved atmospheric downwelling radiances, measured in the 100-1500  $\text{cm}^{-1}$  spectral range with 0.4  $\text{cm}^{-1}$  resolution and a radiometric uncertainty better than 0.85  $\text{mW/m}^2\text{sr cm}^{-1}$ .

## 1 Introduction

The measurement of the atmospheric downwelling longwave radiance (DLR) is a crucial task in climate and Earth radiation budget studies since it provides the complementary quantity to the top-of-atmosphere outgoing longwave radiance (OLR) measured from space. The knowledge of both these quantities is needed in order to achieve a complete characterization of the Earth radiation budget (ERB) (Wild, 2013).

A spectrally resolved measurement of the DLR provides significant advantages with respect to spectrally integrated measurements, allowing for an accurate identification of the radiative signatures, and thus the contributions to the ERB, of the various atmospheric constituents.

On the other hand, spectrally resolved measurements, in order to observe an homogeneous scene, typically provide only the radiance in a small solid angle. Further calculations, or several measurements made at different angles, are needed to estimate the irradiance.

This limitation can be overcome with the use of a radiative transfer model and the application of an inversion procedure on the measured atmospheric emission spectra to retrieve vertical profiles of relevant variables as water vapor, temperature and minor constituents. These variables can be used in the forward model to reconstruct radiance in the lines of sight that were not directly measured (Palchetti, 2017).

This kind of analysis also constitutes, in itself, an alternative monitoring method with respect to radiosounding.

The Radiation Explorer in the Far Infrared - Prototype for Applications and Development (REFIR-PAD) Fourier transform spectroradiometer has been developed with the aim of performing the spectrally resolved measurement of atmospheric emitted



radiation, covering the most part of the atmospheric emission spectrum, from 7 to 100 $\mu\text{m}$ , thus including the far-infrared (FIR) region, defined as wavelengths greater than 15 $\mu\text{m}$  or, approximately, above the CO<sub>2</sub>  $\nu_2$  band.

While the relevance of the FIR spectral interval for atmospheric studies, and in particular for the study of climate, is a well-established concept (Sinha, 1995; Brindley, 1998; Harries, 2008), FIR still remains a significantly underexplored region, even  
5 more if we consider specifically long-term monitoring projects.

The use in the REFIR-PAD instrument of room-temperature detectors and of highly reliable mechanical solutions derived from space-qualified projects (Rizzi, 2002), makes of it an ideal tool to perform monitoring mission on climatologically relevant timescales. This capability has been tested in 2007 with the ECOWAR campaign (Earth COoling by WAter vapor Radiation) (Bhawar, 2008) and in 2009 with the RHUBC-II campaign (Radiative Heating in the Underexplored Bands Campaign - II)  
10 (Turner, 2012). REFIR-PAD measurement capabilities are currently being fully exploited with the installation of the instrument in the Italian-French Antarctic station Concordia, in the Dome C region on the Antarctic Plateau (75° 06' S, 123° 23' E, 3.233 m a. s. l.), where it is operating in continuous acquisition mode since December 2011.

The REFIR-PAD Antarctic campaign is performed in the framework of several research programs financed by the Italian Antarctic Research Program (PNRA - Programma Nazionale di Ricerca in Antartide): PRANA (Proprietà Radiative del va-  
15 pore Acqueo e delle Nubi in Antartide), COMPASS (COncordia Multi-Process Atmospheric StudieS), DOCTOR (DOme C Tropospheric ObserER) and FIRCLOUDS (Far Infrared Radiative Closure Experiment For Antarctic Clouds).

## 2 The REFIR-PAD spectroradiometer

The REFIR-PAD Fourier transform spectroradiometer is based on a Mach-Zehnder interferometer with a folded optical design that allows for a compact instrument while still retaining the moderate resolution and high throughput needed for atmospheric  
20 studies. The folding of the optical path and the number of reflections are designed to provide some degree of scanning mirror misalignment compensation (Carli, 1999a; Palchetti, 1999), allowing for a simpler mirror scanning mechanism design (Bianchini, 2006b).

The Mach-Zehnder configuration provides access to both of the two inputs and the two outputs of the interferometer, allowing for the use of a reference source (Reference Black Body, RBB in Figure 1) permanently installed on the second input, a feature  
25 that as we will see later, is critical for the reduction of beam splitter emission effects. Moreover, output separation allows to have two independent output channels.

The interferometer has the capability of operating both in a Martin-Puplett (Martin, 1969) polarizing scheme, and in a more simple amplitude-division configuration. In the first case, as shown in Figure 1, all the four beam splitters are installed, two acting as polarization divider and recombiner, and the other two, the ones nearer to the mirror scanning mechanism (Roof-Top  
30 Mirror Unit, RTMU in figure), as proper interferometric beam splitters.

The amplitude-division configuration makes use only of the two interferometric beam splitters, while the two other mounts are left empty. This configuration has shown to be the best choice when aiming for a wide operating spectral range, since with the use of bi-layer dielectric beam splitters the instrumental response can be tuned according to the experimental requirements.

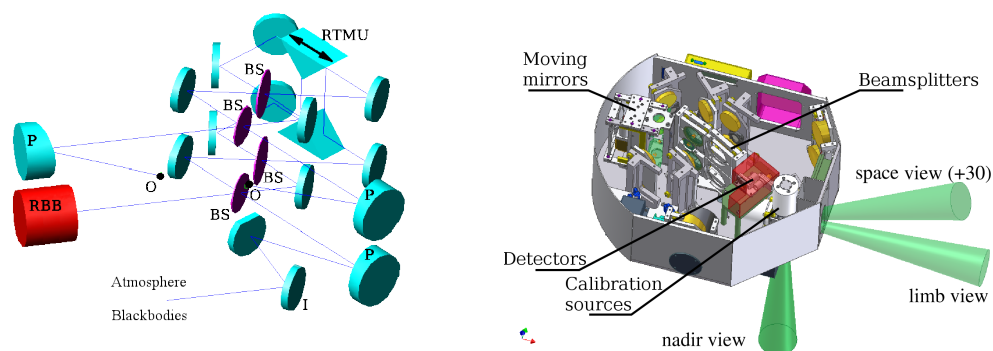


**Figure 1.** Top panel: REFIR-PAD optical layout. BS: beam splitters, P: off-axis parabolic mirrors, RBB: reference blackbody source, O: outputs (detectors), I: input selection mirror, RTMU: roof-top mirror unit (interferometric scanning mirror). Bottom panel: REFIR-PAD layout showing the actual placement of the components in the instrument enclosure.

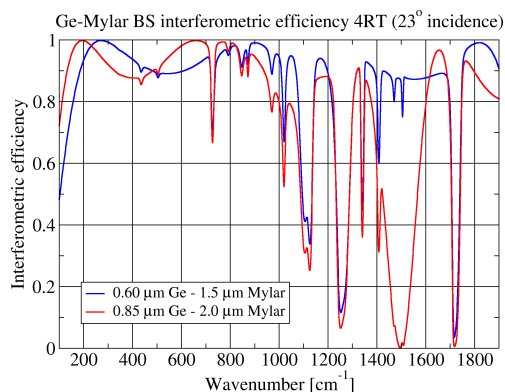


**Figure 2.** Real part of the interferometric efficiency 4RT calculated with two different configurations of the bi-layer Germanium on Mylar substrate beamsplitters.

For example, with a  $0.85 \mu\text{m}$  Ge layer on a  $2 \mu\text{m}$  Mylar substrate an interferometric efficiency better than 80% in the  $100\text{--}1300 \text{ cm}^{-1}$  spectral range can be achieved, while with a thinner structure ( $0.6 \mu\text{m}$  Ge layer on a  $1.5 \mu\text{m}$  Mylar substrate) the response towards higher wavenumbers can be enhanced, extending the operating range to  $1900 \text{ cm}^{-1}$  at the cost of a reduction of the efficiency below  $200 \text{ cm}^{-1}$  (see Figure 2). This does not constitute a problem for ground-based measurements where

5 even in cases of extreme atmospheric transparency, with very low humidity, there is no significant atmospheric signal below  $200\text{--}250 \text{ cm}^{-1}$ .

In Figure 2 is also evident that the substrate itself poses some limitations to the operating spectral range due to its absorption properties. The substrate absorption bands not only reduce the efficiency, possibly “blinding” the instrumental response as in



the case of the strong features near 1250 and 1700  $\text{cm}^{-1}$ , but also introduce a dephasing that makes an accurate radiometric calibration a challenging task in spectral regions close to the absorption bands (Bianchini, 2008a).

These problems could be overcome by using a different substrate, like polypropylene, which has fewer and weaker absorption bands in the region of interest, but this comes at the cost of worse optical and mechanical properties that result critical in the delicate process of beam splitter assembly and Germanium deposition. So Mylar has been chosen as a trade-off between theoretical efficiency and optical quality.

Problems arising from beam splitter substrate absorption, and in general from non-ideal beam splitters are also mitigated through design choices in the interferometer: the use of a reference source (RBB in Figure 1) operating at the same temperature of the instrument, and thus of the beam splitters, reduces ideally to zero the contribution to the interferogram due to beam splitter emission (Carli, 1999b; Bianchini, 2009). The orientation of the two beam splitters is also chosen in order to symmetrize the optical paths and minimize the out-of-phase contributions to the interferogram (Bianchini, 2009). As a matter of fact, the biggest contribution to the interferometer output due to the beam splitters in this configuration comes from the small layer thickness differences between the two beam splitters, differences that are inherent in the manufacturing process.

A rotating folding mirror is placed at the instrument input port, allowing to select an atmospheric line of sight or one of the two on-board calibration sources. The rotating mirror is in the focus of a 320 mm focal length, 20° off-axis parabolic mirror that collimates input radiation towards the interferometer. The second input does not need collimating optics since it is directed towards the large diameter RBB source.

Two 170 mm focal length, 30° off-axis parabolic mirrors focus the interferometer output ports on two 10 mm diameter Winston cone concentrators that feed the detectors. The interferometer is placed in the 1.4 m-length collimated optical path between input and output parabolic mirrors. A 22 mm pupil stop is placed in the center of the collimated path, inside the roof-top mirror unit.

The designed beam divergence  $\Omega$  inside of the interferometer is 0.0027 sr, giving an instrument throughput of 0.011  $\text{cm}^2\text{sr}$ . However in practice there is a limitation that is posed by the concentrator-detector coupling.

The coupling efficiency is limited by the presence of a CsI window that seals the detector case from ambient humidity. Ideally the detector should be placed as near as possible to the concentrator output aperture, but the minimum distance is actually limited by the window thickness and the distance between the window and the detector active surface.

In Figure 3 is shown the variation of the coupling efficiency with the distance between concentrator and detector. The curves corresponding to the two channels differ due to the diameter of the active surface of the two detectors (2 mm for channel 1 and 1.5 mm for channel 2). The dots show the operating condition of the two channels, corresponding to a concentrator-detector distance of 2.7 mm for channel 1 and 2.3 mm for channel 2.

As shown in Figure 3, the limitation in coupling efficiency causes a loss of about 40% in signal, but also acts as a field stop limiting the instrument field of view, reducing the beam divergence to about 0.00087 sr, for a throughput of about 0.0035  $\text{cm}^2\text{sr}$ .

Interferometric metrology is based on a paraxial laser interferometer with a 780 nm laser source (Bianchini, 2000a) that has been thoroughly tested in high-resolution FTS instruments operating both from ground (Palchetti, 2005) and from stratospheric platforms (Bianchini, 2004, 2006a).

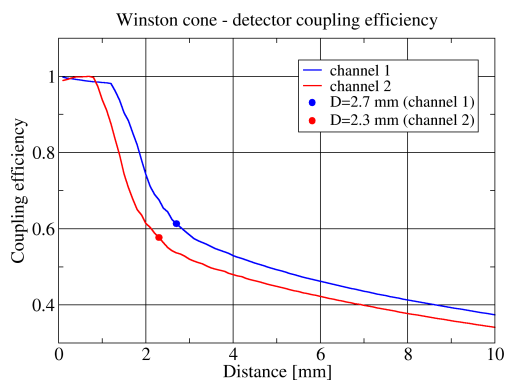


**Figure 3.** Plot of the concentrator-detector coupling efficiency as a function of their distance for both channels. The solid dots show the actual operating point, corresponding to a concentrator-detector distance of 2.7 mm for channel 1 and 2.3 mm for channel 2.

The reference interferometer does not share any of the infrared interferometer optics, simplifying the instrument design and alignment, at the cost of having a possible misalignment between the two optical axes. This doesn't constitute a problem since it induces a linear wavenumber error which is taken care of in the wavenumber calibration procedure. This procedure is based on known atmospheric line centers and does not rely on the measurement of the exact laser wavelength.

- 5 Along with the reference black body RBB, two other black body sources (Palchetti, 2008a) are used for the radiometric calibration of the REFIR-PAD measurements (Bianchini, 2008a). These sources, Hot Black Body (HBB) and Cold Black Body (CBB), are placed near the instrument measurement port and can be switched into the line of sight through the rotating input mirror (see Figure 1, label "Calibration sources"). Acquisition of HBB and CBB can be performed regularly in order to obtain a constant tracking of possible instrumental response function variations. Typically a 10 minutes acquisition sequence
- 10 includes 4 atmospheric measurements and 4 calibrations, 2 with HBB and 2 with CBB. Radiometric performances of the REFIR-PAD instruments are further described in section 5.

### 3 Instrumental line shape

A good model of the instrumental line shape (ILS) is a necessary requirement to correctly interpret the measured spectra and perform the level 2 data analysis (Section 8). Several effects can contribute to distort the ILS from the theoretical

15  $\text{sinc}(2\pi\sigma z_{\text{max}})$  function, where  $z_{\text{max}}$  is the maximum optical path difference. Misalignment of the interferometer and scanning mirror deviations (Bianchini, 2000b) can contribute to the ILS, another possible effect is due to the finite solid angle  $\Omega$  of the radiation propagating inside of the interferometer.

The effect of the finite solid angle is to broaden and shift spectral lines by convolving, in the wavenumber domain, the ideal sinc ILS with a box function extending from 0 to  $\sigma_0\Omega/2\pi$ , where  $\sigma_0$  is the spectral line center (Vanasse, 1967).

- 20 Thus, in the optical path difference domain, the effect gives an additional, wavenumber dependent, apodization term  $\text{sinc}(z\sigma_0\Omega/2)$  to be multiplied by the standard boxcar function extending from  $-z_{\text{max}}$  to  $z_{\text{max}}$ . The dependency on wavenumber of the

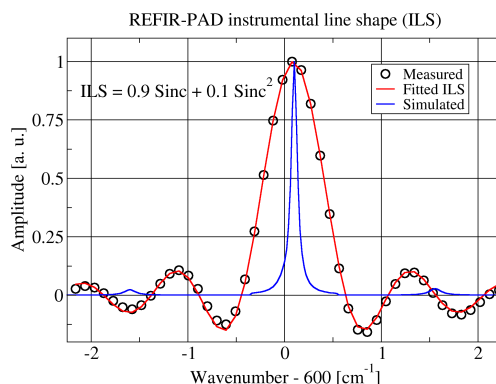


**Figure 4.** REFIR-PAD instrumental line shape. Blue line shows the isolated atmospheric line used for the analysis, the instrumental line shape is a linear combination of sinc and sinc<sup>2</sup> components.

apodization function makes the exact treatment of such an effect a difficult task in the case of a broadband spectrum. A possibility is to consider  $\sigma_0$  a constant, equal to the central wavenumber of the operating spectral band.

Moreover, if  $\pi/\sigma_0\Omega \gg z_{\max}$  the solid angle contribution to the ILS is small, and can be approximated with a triangular component in the apodization. The resulting apodization function can thus be treated as a linear combination of a boxcar and a triangle function with  $\alpha$  and  $1 - \alpha$  coefficients, where  $\alpha = \text{sinc}(z_{\max}\sigma_0\Omega/2)$ .

This is a rough approximation with respect to the exact mathematical treatment of the ILS function, but since in normal instrumental operating conditions the deviations from the “ideal” ILS are very small, the effect of the approximation is negligible, and the calculation of the ILS is much faster since it makes use of the two simplest apodization functions.

REFIR-PAD ILS has been analyzed through hot black body calibration measurements in which an isolated water vapor line coming from residual humidity in the instrument has been identified. The feature is weak enough to be far from saturation, and has a natural linewidth negligible with respect to ILS (see Figure 4, blue line).

The  $\alpha$  coefficient can be also retrieved as a function of wavenumber through the analysis of wide band spectra in which narrow atmospheric lines can be isolated. The result of this kind of analysis is shown in Figure 5, where average  $\alpha$  values are plotted vs. wavenumber for two different series of measurements, performed with a nominal resolution of  $0.25 \text{ cm}^{-1}$  (red circles) and  $0.5 \text{ cm}^{-1}$  (blue squares). The theoretical expression,  $\alpha = \text{sinc}(z_{\max}\sigma_0\Omega/2)$  is also plotted, with an  $\Omega$  value fitted to the experimental data.

Both the datasets provide the same  $\Omega$  value, as expected, also, the fitted value (0.0008 sr) is smaller than the theoretical beam divergence given by the optical design (about 0.0027 sr), but in good agreement with the actual value of 0.00087 sr calculated taking into account the limitations in coupling efficiency due to the finite distance between Winston cones output aperture and detectors (see Section 2).

It should be noted that at low wavenumbers the solid angle contribution is completely negligible, but even in this case, line fitting gives an  $\alpha$  value lower than 1 (typically about 0.95). This can be explained with the fact that there are other

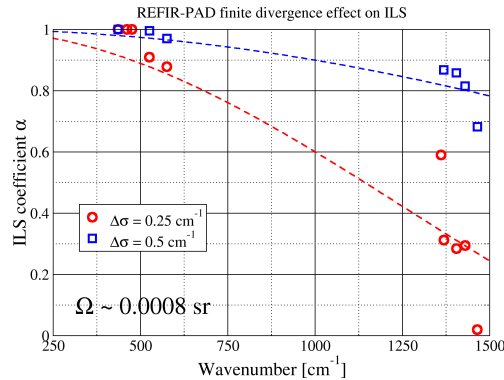


**Figure 5.** REFIR-PAD instrumental line shape coefficient obtained through analysis of measured spectra for 0.25 and 0.5  $\text{cm}^{-1}$  nominal resolution. Continuous lines show the  $\text{sinc}(z_{\text{max}}\sigma_0\Omega/2)$  theoretical behaviour.

contributions to the ILS (residual misalignment, optics planarity, scanning mirror movement irregularities) that can give a residual contribution that is visible when the main effect is negligible.

We also observe that, since in case of a small amount of interferometric misalignment the effect can be approximated at the first order with an increase of the  $\text{sinc}^2$  component, it is possible to treat the interferometric misalignment in level 2 data analysis through fitting the  $\text{sinc}/\text{sinc}^2$  ratio as an extra parameter (see Section 8), a very useful feature in case of remote operation in extreme environments, a situation in which a slight misalignment is always a possibility.

#### 4 Detectors and data acquisition electronics

One of the defining characteristics of the REFIR-PAD spectroradiometer is the use of room-temperature detectors to cover the far to middle-infrared spectral range. This result is obtained through the use of high-sensitivity Deuterated L-Alanine doped Triglycine Sulphate pyroelectric detectors provided by BAE-Selex (models P5315 and P5541). Specifications for the P5315 (P5541) at  $f = 100$  Hz are: Detectivity  $D^* = 5.0 \cdot 10^8 (5.3 \cdot 10^8) \text{ cm}\sqrt{\text{Hz}}/\text{W}$ , Responsivity 1250 (450) V/W.

The detector active area diameter is 2 mm for P5315 and 1.5 mm for P5541. To enhance the light-gathering ability of the detectors, Winston cone concentrators are mounted in front of them.

The detectors are specified for 10-3000 Hz operating frequency range. In standard operating conditions ( $3.3 \cdot 10^{-2} \text{ cm/s}$  OPD scanning speed, 100-1500  $\text{cm}^{-1}$  spectral range) the REFIR-PAD instrument operates in the 3.3-49.5 Hz frequency interval. This is partially outside of the low end of the specified operating range, thus an accurate characterization of the detector system is required.

The typical frequency response of a pyroelectric detector is characterized by “crossed” low and high cutoffs resulting in a strongly frequency-dependent amplitude and phase. The presence of a low frequency cutoff is rather an advantage in an intrinsically AC-coupled application like FT spectroscopy, but, on the other side, a frequency-dependent dephasing constitutes

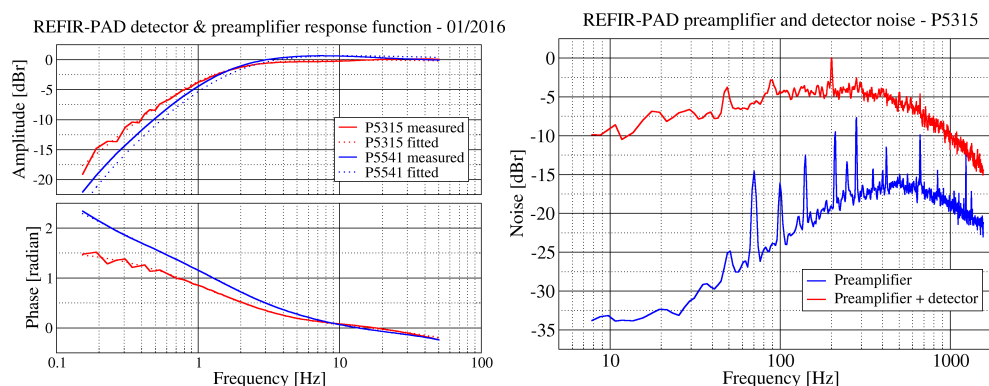


**Figure 6.** Top panel: REFIR-PAD detector preamplifier response as measured in normal operating conditions, along with a fit of the theoretical model used to measure the detectors characteristic low and high pass frequencies. Bottom panel: noise characteristics of the detector and preamplifier system.

a severe problem in a FT spectrometer, and must be solved by the use of a specifically designed preamplifier with a tailored response function in order to obtain a flat response and a very low dephasing across the operating frequency range.

In Figure 6 the main characteristics of the detector and preamplifier system are shown. The response (top panel) is measured in operating conditions, supplying to the detector an optical step function through the use of a laser and a shutter. The resulting response function can be fitted with a mathematical model of the detectors two-pole response multiplied by the preamplifier electronics response in order to obtain an estimate of the actual frequencies of the detector poles. The fitted function is shown in figure as a dotted line, and is in a very good agreement with the measured data.

The values for the low and high frequency cutoffs obtained by the fitting process shown in Figure 6 are used, together with a mathematical simulation of the preamplifier response, to provide an estimate of the residual dephasing to be used in the phase correction algorithm in the processing of interferograms (Bianchini, 2008a).

In the bottom panel of Figure 6 is also shown the noise spectrum at the output of the preamplifier as measured with a Stanford Research SR780 network analyzer, both with and without connecting the detector, showing how in the operating frequency range of the preamplifier (between 1 and 100 Hz) the electronics give a contribution more than 20 dB below the detector noise.

## 5 Radiometric performances

A direct estimate of the radiometric accuracy of the REFIR-PAD spectra can be obtained through the signal measured in a spectral interval in which complete atmospheric transparency is expected.

In the case of a high-altitude, extremely dry environment this condition is achieved in the atmospheric window around 800-1000  $\text{cm}^{-1}$ . Specifically we selected a narrow interval between 828 and 839  $\text{cm}^{-1}$  in which interference due to water vapor lines and minor species is completely negligible.



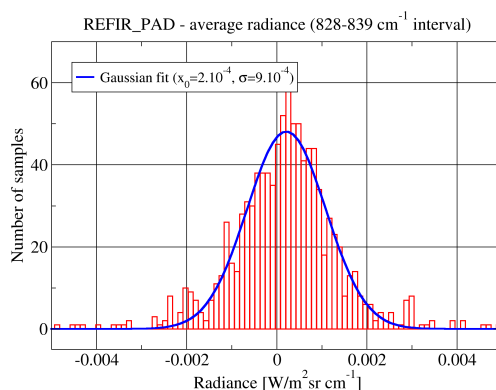


**Figure 7.** Statistical analysis of the average radiometric signal in a high transparency window ( $828\text{--}839\text{ cm}^{-1}$ ). Radiometric bias is estimated in about  $0.2\text{ mW/m}^2\text{sr cm}^{-1}$ , while the half width of the Gaussian distribution is  $0.9\text{ mW/m}^2\text{sr cm}^{-1}$ .

In Figure 7 a statistical analysis of the distribution of the average radiance in the selected interval is presented.

The distribution has been fitted with a Gaussian curve, obtaining a bias of about  $0.2\text{ mW/m}^2\text{sr cm}^{-1}$  and a standard deviation of about  $0.9\text{ mW/m}^2\text{sr cm}^{-1}$ . The latter is in a good agreement with the a-priori estimate of the radiometric error obtained combining the noise equivalent spectral radiance (NESR) and the calibration error (Bianchini, 2008a): the estimated NESR in the selected spectral band is  $<0.6\text{ mW/m}^2\text{sr cm}^{-1}$  and the calibration uncertainty is  $0.6\text{ mW/m}^2\text{sr cm}^{-1}$ , giving a total uncertainty (through root sum of squares) of about  $0.85\text{ mW/m}^2\text{sr cm}^{-1}$ .

The much lower value of constant bias show that systematic errors in the calibration procedure are negligible with respect to the estimated radiometric uncertainty.

## 6 Spectroscopic performances

10 A simulation software has been developed with the intent of providing a tool to better understand the behavior of the REFIR-PAD interferometer. The code is written in MATLAB-compatible language, and takes into account all relevant elements of the instrument geometry and optical design.

The simulation assumes a generic Mach-Zehnder design with two independent inputs and two outputs. The beam splitters are modeled as asymmetric multilayers characterized by generally different optical reflectivities for the two sides  $R_1$ ,  $R_2$ .

15 In the simulation the two inputs can be associated to a blackbody source or to a synthetic spectrum provided by an atmospheric forward model, so in both cases a real function. The two sources are split according to the calculated complex transmission and reflection coefficients of the first beam splitter as obtained by the dielectric multilayer theory using the measured complex refractive indexes for the different layers in order to correctly represent bulk material absorption.

20 The emission of the first beam splitter, due to its non-null absorption, is also considered as an independent source. Beam splitter absorption is mainly caused by the substrate absorption bands, so it appears as a localized and easily identifiable effect.

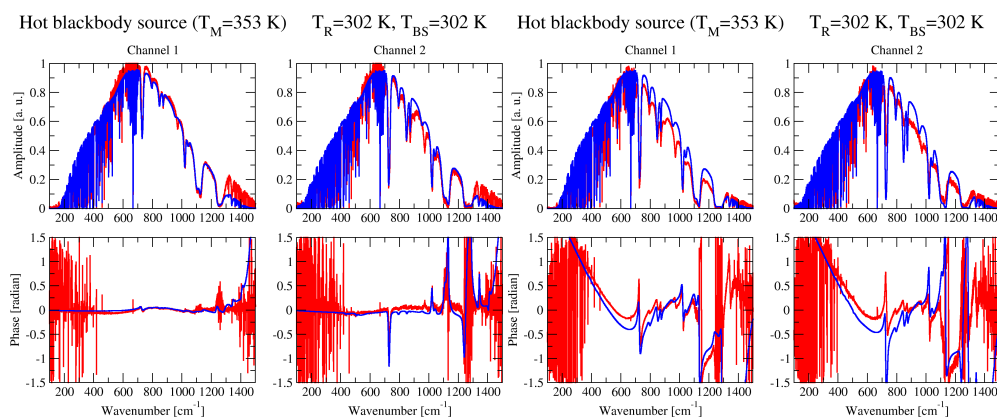


**Figure 8.** Simulation of the REFIR-PAD instrumental response function for different beamsplitter setups (blue line). Compensated (top 4 panels) and unbalanced (bottom 4 panels) configurations are shown. Laboratory measurements (red line) are compared with simulation outputs for the corresponding configuration.

The two arms of the interferometer are then recombined on the second beam splitter whose properties are calculated in the same way as for the first.

Effect of the misalignment of interferometric components is calculated in the circular beam approximation using Bessel functions, planarity error is also modeled using simple approximations (spherical or trapezoidal deformation) and integrated on the beam profile.

The resulting complex spectrum is multiplied for a real absorption spectrum simulating the effect of air inside of the instrument (most of the absorption takes place outside of the interferometric path thus it doesn't produce dephasing) and the effect of the detector windows, obtaining the total signal incoming on both detectors. An inverse Fourier transform is applied to this signal to generate the simulated interferogram, which is then processed with the standard data analysis chain used to process the REFIR-PAD measurements.

In Figure 8 a simulation of an acquisition of the internal hot blackbody source is shown. All the relevant features of the measured spectrum are well represented in the simulation, including the substrate absorption bands between 700 and 1400  $\text{cm}^{-1}$ , and the minimum in interferometric efficiency near 1500  $\text{cm}^{-1}$  that is due to the periodical characteristic of multilayer beam splitters (the tests were performed with the 0.85  $\mu\text{m}$  Ge on 2.0  $\mu\text{m}$  Mylar beamsplitters). Actually the minimum is split in two due to small differences in thickness between the two beam splitters, a behavior that is also correctly modeled.

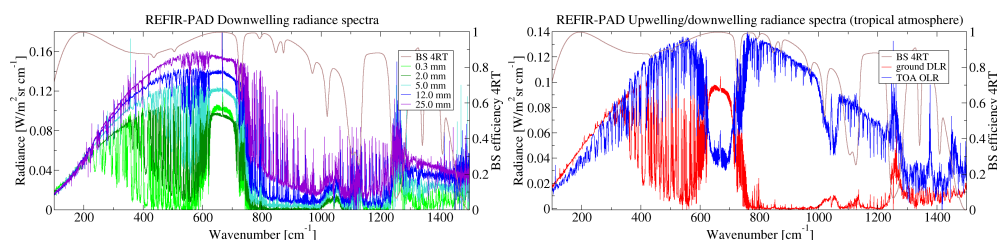


**Figure 9.** REFIR-PAD level 1 data products. Top panel: average zenith-looking spectra corresponding to about 6 h of data acquisition obtained in different atmospheric humidity conditions, spanning about two order of magnitude in terms of total precipitable water vapor (PWV). Beam splitter efficiency curve is also shown, to explain noise bands. Bottom panel: ground-based zenith-looking spectrum compared with top of atmosphere, nadir-looking measurement performed in tropical regions.

## 7 Level 1 products

The main data product of the REFIR-PAD spectroradiometer is the atmospheric emitted radiance integrated in the field of view of the instrument (a cone with an aperture of about  $10^\circ$ ), spectrally resolved with a  $0.4 \text{ cm}^{-1}$  resolution in the  $100\text{--}1500 \text{ cm}^{-1}$  range.

- 5 The REFIR-PAD spectroradiometer has been operated in several campaigns in different environments (tropical, midlatitude, polar), and at different working altitudes, from about sea level to over 5000 m a.s.l. (Bianchini, 2007; Bhawar, 2008; Turner, 2012; Palchetti, 2015).

In Figure 9, top panel, a set of calibrated spectra acquired in different atmospheric conditions is shown. Each spectrum correspond to an average of about 6 h of measurement in clear sky conditions. The measurements span about 2 orders of magnitude in terms of atmospheric total precipitable water vapor (PWV).

The REFIR-PAD instrument has also been operated in nadir-looking observation mode from stratospheric balloon platform (Palchetti, 2006), obtaining atmospheric emission spectra from a 38 km altitude, thus assimilable, for practical purposes, to the top of atmosphere (TOA) condition. In Figure 9, bottom panel is shown a comparison between the TOA spectrum acquired during the flight and a ground-based zenith-looking measurement performed in similar condition (tropical atmosphere).

- 15 The measured spectral range includes almost all of the thermal emission from the Earth's atmosphere. If we consider the far-infrared region ( $200\text{--}667 \text{ cm}^{-1}$ ), that is the main scientific target of the REFIR-PAD instrument, using the radiometric accuracy figures provided in Section 5 and the spectra shown in Figure 9, we obtain a relative uncertainty in the measurement of the total radiance between 0.7% and 2%.

## 8 Level 2 products

- 20 The REFIR-PAD level 1 data products can provide plenty of information not only on the radiative properties of the atmosphere, but also on its structure and composition. To perform the retrieval of these variables, a software has been developed (Bianchini,

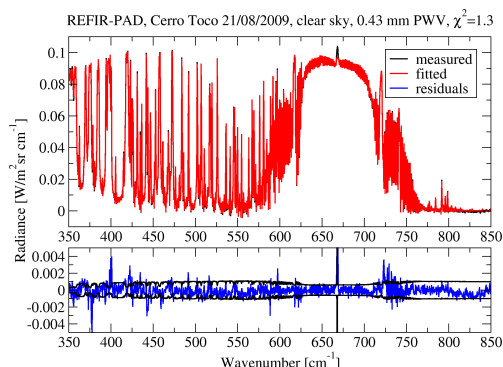


**Figure 10.** A typical result of the level 2 data analysis process. A single REFIR-PAD measurement is fitted using the LBLRTM forward model and the MINUIT minimization routines. Fitting residuals are compared with the total radiometric uncertainty (black line) in the bottom panel.

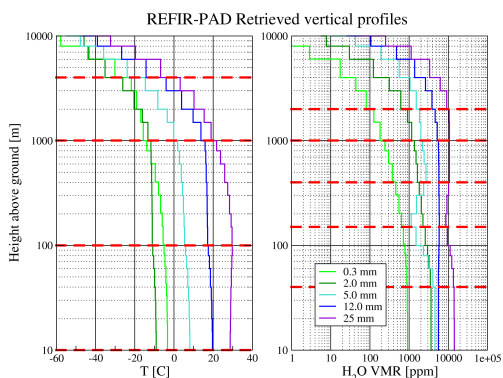


**Figure 11.** Vertical temperature and water vapor profiles obtained from the spectra in Figure 9, top panel, through the level 2 data analysis process. Red dashed lines show the selected fitting layers for temperature and water vapor.

2011) that is based on the Line-By-Line Radiative Transfer Model (LBLRTM) (Clough, 2005) and the MINUIT minimization routines, part of the CERNlibs.

The software allows to retrieve temperature and water vapor content on separate vertical grids, together with extra parameters like columnar amounts of minor species, cloud optical thickness and instrumental parameters (wavenumber calibration shift, instrumental line shape factor).

A typical retrieval operates on a 4-point grid for temperature and a 5-point grid for water vapor, with retrieval levels chosen on the base of an analysis of the Jacobians of the selected variables. In Figure 10 the typical result of a fitting process is shown.

The vertical profiles of temperature and humidity obtained from the analysis of the set of zenith-looking measurement shown in Figure 9, top panel, are presented in Figure 11. These results show how the process can operate in a very wide range of atmospheric conditions.



In order to better reflect the atmospheric modeling performed by LBLRTM the fitted profiles are shown as histograms following the layering structure adopted in the forward model. The logarithmic scale adopted for the representation of the vertical profile reflects the logarithmic spacing used in the layering, which derives from the decrease of vertical resolution with height that is inherent in the zenith-looking vertical sounding geometry.

5 The PWV is also provided as a level 2 data product, the accuracy in the determination of the PWV depends on the atmospheric conditions (total amount of water, presence of clouds) and ranges from 10-20% in the extremely dry conditions found in Antarctica to about 5% in mid-latitude atmosphere.

Columnar amount of other tropospheric minor species with spectral lines in the REFIR-PAD measurement range can be retrieved, nitrous oxide for example. Methane also could be easily retrieved, but its main feature lies on the absorption band  
10 of the Mylar beam splitter substrate, so a different beam splitter design (e. g. using Polypropylene) would be needed for an efficient methane total column retrieval.

A different consideration must be made for ozone column retrieval: while a strong ozone emission band is present in the REFIR-PAD operating spectral interval, most of the ozone lies in the stratosphere where the temperature retrieval, mainly relying on the Carbon Dioxide  $\nu_2$  band, has no sensitivity. Thus to correctly interpret the emitted radiance due to the ozone  
15 band, stratospheric temperatures must be provided as an external input. This can be done through radiosounding, or through an auxiliary sensor as a stratospheric Raman LIDAR (Bianchini, 2014).

## 9 Conclusions

The REFIR-PAD spectroradiometer has proved to be a reliable and relatively simple tool for the remote sensing of the radiative properties, composition and thermal structure of the troposphere, providing a wealth of information with a measurement repetition rate of the order of 10 minutes, fast enough to resolve all the relevant atmospheric processes. The provided data products  
20 are:

- Atmospheric emitted radiance spectra in the 100-1500  $\text{cm}^{-1}$  range with 0.4  $\text{cm}^{-1}$  resolution and 0.85  $\text{mW/m}^2\text{sr cm}^{-1}$  accuracy.
- Tropospheric water vapor and temperature vertical profiles with up to 5 independently fitted points.
- 25 – Total columnar precipitable water vapor (PWV) with an accuracy ranging from 5% to 20% depending on the total humidity and atmospheric conditions.
- Columnar amounts of minor species as nitrous oxide, methane and ozone.
- Cloud optical thickness in the atmospheric transparency window region (800-1200  $\text{cm}^{-1}$ ).

The instrument operates at room temperature, is fully autonomous and allows for remote control of all relevant settings, thus  
30 is perfectly suitable for operation in remote and extreme environment, as demonstrated by more than 6 years of continuous operation in the Antarctic station Concordia.



It should be noted that this specific location provides itself an unique dataset, since no similar instruments are operating continuously in polar regions.

*Acknowledgements.* We would like to acknowledge the Italian Antarctic Program, Programma Nazionale di Ricerca in Antartide (PNRA) for the funding for the following research programs, that have allowed to perform REFIR-PAD measurements since December 2011 at Concordia  
5 Station, Antarctica: project PRANA (Proprietà Radiative del vapore Acqueo e delle Nubi in Antartide) 2009/A04.03 2011-2013, project COMPASS (COncordia Multi-Process Atmospheric StudieS) 2013/AC3.01 2013-2016, and the currently active projects DOCTOR (DOme C Tropospheric ObserveR) 2016/AC3.02 and FIRCLOUDS (Far Infrared Radiative Closure Experiment For Antarctic Clouds) 2016/AC3.03.



## References

- Bianchini, G., Lanfranchi, M., and Cortesi, U.: Flight qualification of a diode laser for path difference determination of a high-resolution Fourier transform spectrometer, *Appl. Optics*, 39, 962–965, 2000a.
- Bianchini, G., and Raspollini, P.: Characterization of instrumental line shape distortions due to path difference dependent phase errors in a Fourier transform spectrometer, *Infr. Phys. Techn.*, 41, 287–292, 2000b.
- 5 Bianchini, G., Cortesi, U., Palchetti, L., and Pascale, E.: SAFIRE/A (spectroscopy of the atmosphere by far-infrared emission - airborne): optimised instrument configuration and new assessment of improved performances, *Appl. Optics*, 43, 2962–2977, 2004.
- Bianchini, G., Boscaleri, A., Carli, B., Mencaraglia, F., Palchetti, L., Pascale, E.: IBEX (Infrared Balloon Experiment): improved instrumental configuration and assessment of instrument performances, *Appl. Optics*, 45, 1041–1051, 2006a.
- 10 Bianchini, G., Castagnoli, F., Pellegrini, M., and Palchetti, L.: Frictionless mirror drive for intermediate resolution infrared Fourier transform spectroscopy, *Infr. Phys. Techn.*, 48, 217–222, 2006b.
- Bianchini, G., Palchetti, L., Baglioni, A., and Castagnoli, F.: Far-infrared spectrally resolved broadband emission of the atmosphere from Morello and Gomito mountains near Florence, *Remote Sensing of Clouds and the Atmosphere XII*, edited by A. Comerón, R. H. Picard, K. Schäfer, J. R. Slusser, A. Amodio, *Proc. SPIE*, 6745, 674518, 2007.
- 15 Bianchini, G., and Palchetti, L.: Technical Note: REFIR-PAD level 1 data analysis and performance characterization, *Atmos. Chem. Phys.*, 8, 3817–3826, 2008a.
- Bianchini, G., Carli, B., Cortesi, U., Del Bianco, S., Gai, M., and Palchetti, L.: Test of far infrared atmospheric spectroscopy using wide-band balloon borne measurements of the upwelling radiance, *J. Quant. Spectrosc. Ra.*, 109, 1030–1042, doi: 10.1016/j.jqsrt.2007.11.010, 2008b.
- 20 Bianchini, G., Palchetti, L., and Carli, B.: Vectorial combination of signals in Fourier transform spectroscopy, *Infr. Phys. Techn.*, 52, 19–21, doi: 10.1016/j.infrared.2008.09.004, 2009.
- Bianchini, G., Palchetti, L., Muscari, G., Fiorucci, I., Di Girolamo, P., and Di Iorio, T.: Water vapor sounding with the far infrared REFIR-PAD spectroradiometer from a high-altitude ground-based station during the Ecowar campaign, *J. Geophys. Res.*, 116, D02310, doi:10.1029/2010JD014530, 2011.
- 25 Bianchini, G., Argentini, S., Baldi, M., Cairo, F., Calzolari, F., Casasanta, G., Conidi, A., Del Guasta, M., Di Natale, G., Federico, S., Lupi, A., Mazzola, M., De Muro, M., Palchetti, L., Petenko, I., Petkov, B., Snels, M., Trivellone, G., Viola, A., and Viterbini, M.: Concordia Multi-Process Atmospheric Studies (CoMPASs): study of the vertical structure of the Antarctic atmosphere with a synergy of different remote sensing techniques, *EGU General Assembly Conference Abstracts*, 16, 7782, 2014.
- Bhawar, R., Bianchini, G., Bozzo, A., Calvello, M. R., Cacciani, M., Carlotti, M., Castagnoli, F., Cuomo, V., Di Girolamo, P., Di Iorio, T., Di Liberto, L., di Sarra, A., Esposito, F., Fiocco, G., Fuà, D., Grieco, G., Maestri, T., Masiello, G., Muscari, G., Palchetti, L., Papandrea, E., Pavese, G., Restieri, R., Rizzi, R., Romano, F., Serio, C., Summa, D., Todini, G., and Tosi, E.: Spectrally Resolved Observations of Earth's Emission Spectrum in the H<sub>2</sub>O Rotation Band, *Geophys. Res. Lett.*, 35, L04812, doi: 10.1029/2007GL032207, 2008.
- Brindley H. E., and Harries, J. E.: The impact of far I. R. absorption on clear sky greenhouse forcing: sensitivity studies at high spectral resolution, *J. Quant. Spectrosc. Ra.*, 60, 151–180, 1998.
- 35 Carli, B., Barbis, A., Harries, J. E., and Palchetti, L.: Design of an efficient broad band far infrared FT spectrometer, *Appl. Optics*, 38, 3945–3950, 1999a.



- Carli, B., Palchetti, L., and Raspollini, P.: Effect of beam splitter emission in Fourier-transform spectroscopy, *Appl. Optics*, 38, 7475–7480, 1999b.
- Clough, S. A., Shephard, M. W., Mlawer, E. J., Delamere, J. S., Iacono, M. J., Cady-Pereira, K., Boukabara, S., and Brown, P. D.: Atmospheric radiative transfer modeling: a summary of the AER codes: Short communication, *J. Quant. Spectrosc. Ra.*, 91, 233–244, 2005.
- 5 Esposito, F., Grieco, G., Leone, L., Restieri, R., Serio, C., Bianchini, G., Palchetti, L., Pellegrini, M., Cuomo, V., Masiello, G., and Pavese, G.: REFIR/BB initial observations in the water vapour rotational band: results from a field campaign, *J. Quant. Spectrosc. Ra.*, 103, 524–535, doi: 10.1016/j.jqsrt.2006.07.006, 2006.
- Fiorucci, I., Muscari, G., Bianchi, C., Di Girolamo, P., Esposito, F., Grieco, G., Summa, D., Bianchini, G., Palchetti, L., Cacciani, M., Di Iorio, T., Pavese, G., Cimini, D., and de Zafra, R. L.: Measurements of low amounts of precipitable water vapor by mm-wave spectroscopy: an intercomparison with radiosonde, Raman Lidar and FTIR data, *J. Geophys. Res.*, 113, D14314, doi: 10.1029/2008JD009831, 2008.
- 10 Harries, J. E., Carli, B., Rizzi, R., Serio, C., Mlyneczek, M., Palchetti, L., Maestri, T., Brindley, H., and Masiello, G.: The Far-Infrared Earth, *Rev. Geophys.*, 46, RG4004, 2008.
- Martin D. H., and Puppert, E.: Polarised interferometric spectrometry for the millimetre and submillimetre spectrum, *Infr. Phys. Techn.*, 10, 105–109, 1969.
- 15 Palchetti, L., Barbis, A., Harries, J. E., and Lastrucci, D.: Design and mathematical modelling of the space-borne far-infrared Fourier transform spectrometer for REFIR experiment, *Infr. Phys. Techn.*, 40, 367–377, 1999.
- Palchetti, L., and Lastrucci, D.: Spectral noise due to sampling error in Fourier transform spectroscopy, *Appl. Optics*, 40, 3235–3243, 2001.
- Palchetti, L., Bianchini, G., Castagnoli, F., Carli, B., Serio, C., Esposito, F., Cuomo, V., Rizzi, R., and Maestri, T.: Breadboard of a Fourier-transform spectrometer for the Radiation Explorer in the Far Infrared atmospheric mission, *Appl. Optics*, 44, 2870–2878, 2005.
- 20 Palchetti, L., Belotti, C., Bianchini, G., Castagnoli, F., Carli, B., Cortesi, U., Pellegrini, M., Camy-Peyret, C., Jeseck, P., and Tè, Y.: Technical note: First spectral measurement of the Earth’s upwelling emission using an uncooled wideband Fourier transform spectrometer, *Atmos. Chem. Phys.*, 6, 5025–5030, 2006.
- Palchetti, L., Bianchini, G., and Castagnoli, F.: Design and characterisation of black-body sources for infrared wide-band Fourier transform spectroscopy, *Infr. Phys. Techn.*, 51, 207–215, doi: 10.1016/j.infrared.2007.06.001, 2008a.
- 25 Palchetti, L., Bianchini, G., Carli, B., Cortesi, U., and Del Bianco, S.: Measurement of the water vapour vertical profile and of the Earth’s outgoing far infrared flux, *Atmos. Chem. Phys.*, 8, 2885–2894, 2008b.
- Palchetti, L., Bianchini, G., Di Natale, G., and Del Guasta, M.: Far infrared radiative properties of water vapor and clouds in Antarctica, *Bull. Am. Meteorol. Soc.*, 96, 1505–1518, doi:10.1175/BAMS-D-13-00286.1, 2015.
- Palchetti, L., Lanconelli, C., Bianchini, G., and Di Natale, G.: Spectral characterization of the surface longwave radiation over the East Antarctic Plateau, *AIP Conf. Proc.*, 1810, 100005, 2017.
- 30 Rizzi, R., Palchetti, L., Carli, B., Bonsignori, R., Harries, J. E., Leotin, J., Peskett, S., Serio, C., and Sutera, A., Feasibility study of the space-borne Radiation Explorer in the Far InfraRed (REFIR), in *Optical Spectroscopic Techniques, Remote Sensing and Instrumentation for Atmospheric and Space Research IV*, A. M. Larar and M. G. Mlyneczek, eds, *Proc. SPIE*, 4485, 202–209, 2002.
- Serio, C., Masiello, G., Esposito, F., Di Girolamo, P., Di Iorio, T., Palchetti, L., Bianchini, G., Muscari, G., Pavese, G., Rizzi, R., Carli, B., and Cuomo, V.: Retrieval of foreign-broadened water vapor continuum coefficients from emitted spectral radiance in the H<sub>2</sub>O rotational band from 240 to 590 cm<sup>-1</sup>, *Opt. Express*, 16, 15816–15833, doi: 10.1364/OE.16.015816, 2008.
- Sinha A., and Harries, J. E.: Water vapor greenhouse trapping: The role of the far infrared absorption, *Geophys. Res. Lett.*, 22, 2147–2150, 1995.





- Turner, D. D., Mlawer, E. J., Bianchini, G., Cadetdu, M. P., Crewell, S., Delamere, J. S., Knuteson, R. O., Maschwitz, G., Mlynzcak, M., Paine, S., Palchetti, L., and Tobin, D. C., Ground-based high spectral resolution observations of the entire terrestrial spectrum under extremely dry conditions, *Geophys. Res. Lett.*, 39, L10801, doi:10.1029/2012GL051542, 2012.
- Vanasse, G. A., and Sakai, H., VII Fourier Spectroscopy, *Progress in Optics*, edited by E. Wolf, 6, 259–330, 1967.
- 5 Wild, M., Folini, D., Schär, C., Loeb, N., Dutton, E. G., and König-Langlo, G.: The global energy balance from a surface perspective, *Clim. Dyn.*, 40, 3107–3134, 2013.